35th Annual International Conference of the IEEE EMBS
Osaka, Japan, 3 - 7 July, 2013

Effects of the rates of pseudo-spontaneous spikes generated by electric stimuli on information transmission in an auditory nerve fiber model

Parichat Kumsa, *Student Member IEEE*, and Hiroyuki Mino, *Senior Member IEEE*

***Abstract*— In this study, the effects of the rate of pseudo-spontaneous spikes on information transmission of the spike trains in response to the electric pulsatile stimulus currents in an auditory nerve fiber (ANF) model is investigated through computer simulation. The pseudo-spontaneous spikes can be generated by high rate pulsatile electric stimuli, making it possible to efficiently encode sound stimuli into the spike trains of the ANF in cochlear prostheses. In this investigation, the information rate of the spike trains in response to sinusoidally modulated pulsatile electric stimuli was estimated as the amplitude of the pulsatile electric stimuli (the rate of pseudo-spontaneous spikes) was varied. The results show that the information rates increased, reached a maximum, and then decreased, in several different values of modulation depth, as the rate of pseudo-spontaneous spikes increased. This may imply a resonance phenomenon dependent on the rate of pseudo-spontaneous spikes generated by electric stimuli in the ANF model. These findings may play a key role in the design of better cochlear prostheses.**

***Index Terms*— Neural Spike Trains, Pseudo-spontaneous Spikes, Auditory Nerve Fiber Model, Stochastic Hodgkin-Huxley Model, Stochastic Resonance, Cochlear Prostheses**

I. INTRODUCTION

Spontaneous spikes refer to action potentials fired even without any stimulus in nervous systems. The spontaneous spike firings are usually specified quantitatively by the rate of spikes, the count of action potentials per unit time in which the time intervals between them are characterized approximately by the exponential probability density function with a dead time (absolute refractory period) [1], [2]. Although the spontaneous spikes are supposed to be detrimental to information transmission of spike trains due to its randomness, it has been reported in [3], [4], [5], [6], [7], [8], [9] that several tens of spontaneous spikes were observed in an auditory nerve fiber of cats, suggesting that they would play a key role in relaying sounds into cochlear nucleus in the brain stem.

Regarding a particular importance of spontaneous spikes, Rubinstein et al. [10] has proposed a stimulating strategy for cochlear implants to improve the quality of encoding sound stimuli into spike trains in the auditory nerves with the pulsatile electric stimuli generating a pseudo-spontaneous activity. Litvak et al. [11] has reported that the pseudo-spontaneous activity improved the encoding characteristics of sound stimuli in computer simulations and feline experiments. Miller et al. [12] has investigated an influence of spontaneous spike rate on temporal properties of spikes and across-fiber synchrony. Recently, Kumsa and Mino [13] have reported the effects of the spontaneous spike rates generated by inner hair cell synaptic vesicle secretions on information transmission of the spike trains in the ANF model.

Up to now, however, it has been unclear how the rate of the pseudo-spontaneous spikes generated by high rate pulsatile electric stimuli can affect information transmission of the spike trains in the ANF model. Thus, the objective of this research was to investigate, through computer simulation, how the rate of pseudo-spontaneous spikes would affect the properties of encoding the sinusoidal functions into the spike trains and information transmission.

II. METHODS

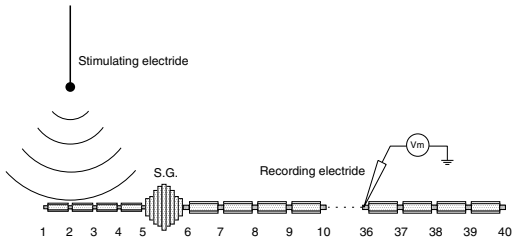

Fig. 1. Auditory nerve fiber model : there is a spiral ganglion (S.G.) with a diameter of 27 μm on the center. This ANF model possesses 40 nodes of Ranvier, and consists of 400 compartments. The axon of the central side is assumed to be connected to cochlear nucleus in brain stem. A stimulating electrode is located at a distance of 1 *mm* above the second node of Ranvier. The transmembrane potentials were recorded at the 36-th node of Ranvier. Note that this figure is not scaled in length.

The ANF model consisting of a spiral ganglion with a diameter of 27 μm possesses 40 nodes of Ranvier with stochastic sodium and potassium channels, implemented by the channel number tracking algorithm [14], and totally 400 compartments as shown in Fig. 1. Figure 1 also shows that a stimulating electrode is located at a distance of 1 *mm* above the second node of Ranvier, whereas the transmembrane potentials were recorded at the 36-th node of Ranvier. We note that this figure is not scaled in length.

The membrane potentials as functions of time t and space k can be expressed as a set of partial difference equations of the diffusion type. In practical situations, the continuous system was solved numerically by digital computers (For more detail, See [15],[16]). In computer simulations, the membrane potentials $V_m^{[k]}(t)$ were solved numerically by the

P. Kumsa is with Graduate School of Engineering, Kanto Gakuin University, 1-50-1 Mutsuura E., Kanazawa-ku, Yokohama 236-8501, Japan, H. Mino is with Department of Electrical and Computer Engineering, Kanto Gakuin University, 1-50-1 Mutsuura E., Kanazawa-ku, Yokohama 236-8501, Japan mino@ieee.org

Crank-Nicholson method [17] at a sampling step (Δt) of 2 μs.

The electric stimuli were applied to a stimulating electrode located at a distance of 1 mm above the second node of Ranvier. The stimulating current was a periodic pulsatile (anodic and cathodic) waveform, and were modulated by a sinusoidal function at a frequency of 440 Hz with a modulation depth, m, of 1, 2.5, 5, 7.5, or 10 % [11] expressed as :

$$I_{ele}(t) = I_{pulse}(t)\{1 + \frac{m}{100} sin(2\pi ft + \Phi)\} \quad (1)$$

where f stands for the sinusoidal frequency, Φ denotes a randomized initial phase taking a value between 0 and 2π and where

$$I_{pulse}(t) = \begin{cases} I_p \sum_{n=0} \{u(t - n\tau_{int}) - 2u(t - w - n\tau_{int}) \\ \qquad +u(t - 2w - n\tau_{int})\} \\ \qquad (n\tau_{int} \le t < n\tau_{int} + 2w) \\ 0 \qquad (otherwise) \end{cases} \quad (2)$$

where I_p denotes the amplitude of pulsatile stimuli, and w=40μs, τ_{int}=200μs (5 kHz), and in which $u(t)$ denotes a unit step function as follows :

$$u(t) = \begin{cases} 1 & (0 \le t) \\ 0 & (otherwise) \end{cases} \quad (3)$$

The sinusoidal component was added after 10 ms in simulation time for numerical stability.

The information rates of the spike trains recorded at the 36th node of Ranvier was estimated by calculating the total entropy and the noise entropy [19], [18], from the inter-spike interval of spike firing times, T, as follows [20],[16] :

$$I_{rate}(T, I_{ele}(t)) = R[H(T) - H(T|I_{ele}(t))] \quad (4)$$

where

$$H(T) = -\sum_{i=0}^{\infty} p(T_i) log_2 P(T_i)$$

$$H(T|I_{ele}(t)) = -E[\sum_{i=0}^{\infty} p(T_i|I_{ele}(t)) log_2 p(T_i|I_{ele}(t))]$$

in which $H(T)$ and $H(T|(I_{ele}(t))$ denote the total entropy of inter spike intervals (ISIs), and the noise entropy of ISIs, given the condition on the stimulus current, $I_{ele}(t)$. R stands for spike rates, and $E[\,]$ designates the expectation operation.

III. RESULTS

Since the rate of pseudo-spontaneous spikes has been known to be dependent upon the amplitude of electric pulsatile stimuli, I_p in (2), the relationship between the rate of pseudo-spontaneous spikes, denoted by $\hat{\lambda}_{p-spon}$, and the amplitude of stimuli was investigated in the ANF model presented in this paper, as shown in Figure 2.

In electric stimulation, the amplitude of pulsatile waveform, I_p, was varied to see how the rate of pseudo-spontaneous spikes, $\hat{\lambda}_{p-spon}$, would affect the properties of encoding the sinusoidal functions into the spike trains and the information transmission.

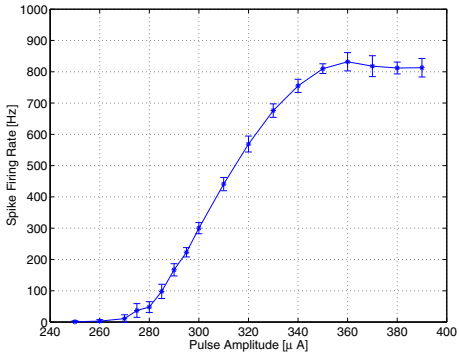

Fig. 2. Spike firing rates as a function of the amplitude of pulsatile waveform, as described in (2), at a duration of 40 μs and a period of 200 μs (5 kHz). Each point was plotted by mean $\pm$ standard deviation bar calculated from 10 samples.

Figure 3 depicts the electric pulsatile stimulus currents as a function of time, $I_{ele}(t)$, (top trace), raster plots of 300 trials (middle trace), the PSTH (bottom trace) with a bin width of 0.5 ms at I_p= 266 μA ($\hat{\lambda}_{p-spon}$=7 [s^{-1}]), m=5 %, and f=440 Hz. The pulsatile waveform was modulated by a sinusoidal function at 440 Hz after 10 ms. In this figure, the raster plot does not seem to synchronize to a frequency of 440 Hz. It was observed that the sinusoids were not necessarily encoded well into the spike trains, because the PSTH was not agreed with the modulated waveform.

When the amplitude of pulsatile waveform, I_p, was set at 271 μA ($\hat{\lambda}_{p-spon}$=14 [s^{-1}]), the raster plot shows that the sinusoids at a frequency of 440 Hz look like better encoded into the spike trains, compared to those in Figure 4. The modulation depth was set at 5 %.

As the amplitude of pulsatile waveform, I_p, was increased, the number of spontaneous spikes tended to increase, as shown in the raster plot of Figure 5 at I_p= 279 μA ($\hat{\lambda}_{p-spon}$=46 [s^{-1}]), m=5 %, and f = 440Hz. The figure shows that the unwanted spike firings other than those modulated by the sinusoids of 440 Hz were observed, implying that a much greater value of spontaneous spike rates could make it difficult to encode accurately the sinusoidal information into the spike trains.

Since the raster plot and PSTH could not provide us with any quantitative measure in electric stimulation, we evaluated quantitatively the information rates of the spike trains in response to the electric pulsatile stimulus currents, modulated by sinusoidal functions.

The information rates were estimated according to (4) in which the mutual information was estimated from observations of the ISI histograms, as the amplitude of electric pulsatile stimulus currents, I_p, were varied. Figures 6-8 show the ISI histograms, with a bin width of 0.5 ms, used in estimating the total entropy, when I_p's were set at I_p=266 μA ($\hat{\lambda}_{p-spon}$=7 s^{-1}) in Figure 6, 271 μA ($\hat{\lambda}_{p-spon}$=14 s^{-1}) in Figure 7, and 279 μA ($\hat{\lambda}_{p-spon}$=46 s^{-1}) in Figure 8 and the frequency and modulation depth were set as follows : f=440 Hz, m=5 %.

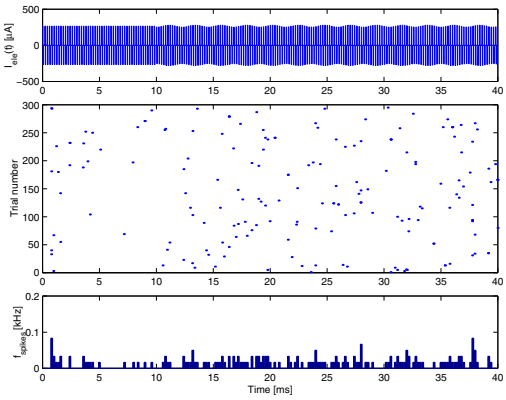

Fig. 3. Stimulating waveform as a function of time, $I_{ele}(t)$, (top trace), Raster plots of 300 trials (middle trace), Post-stimulus time histogram with a bin width of 0.5 *ms* (bottom trace) at I_p=266 μA ($\hat{\lambda}_{p-spon}$=7 s^{-1}) and f=440 Hz, m=5 %

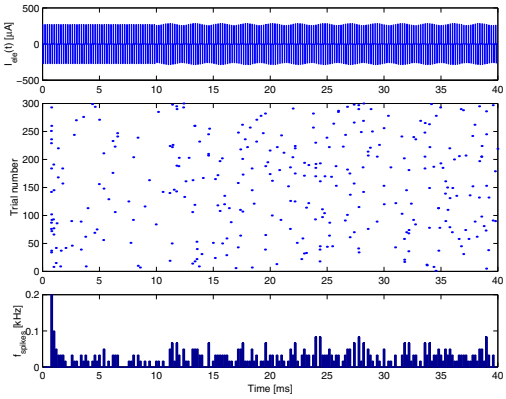

Fig. 4. Stimulating waveform as a function of time, $I_{ele}(t)$, (top trace), Raster plots of 300 trials (middle trace), Post-stimulus time histogram with a bin width of 0.5 *ms* (bottom trace) at I_p=271 μA ($\hat{\lambda}_{p-spon}$=14 s^{-1}) and f=440 Hz, m=5 %

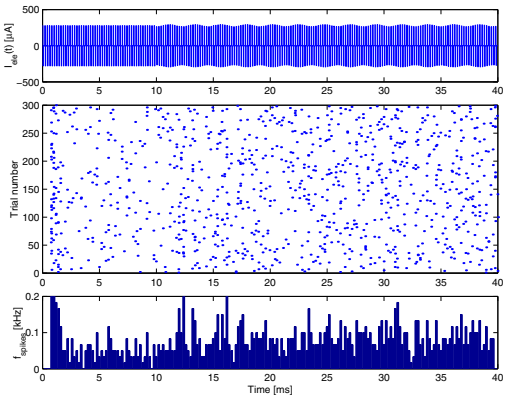

Fig. 5. Stimulating waveform as a function of time, $I_{ele}(t)$, (top trace), Raster plots of 300 trials (middle trace), Post-stimulus time histogram with a bin width of 0.5 *ms* (bottom trace) at I_p=279 μA ($\hat{\lambda}_{p-spon}$=46 s^{-1}) and f=440 Hz, m=5 %

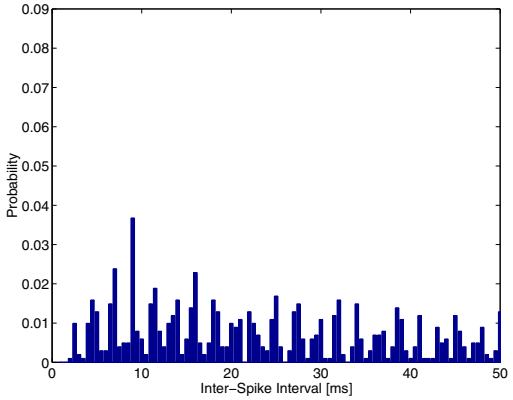

Fig. 6. Inter-Spike Interval histograms with a bin width of 0.5 *ms* at I_p=266 μA ($\hat{\lambda}_{p-spon}$=7 s^{-1}) and f=440 Hz, m=5 %

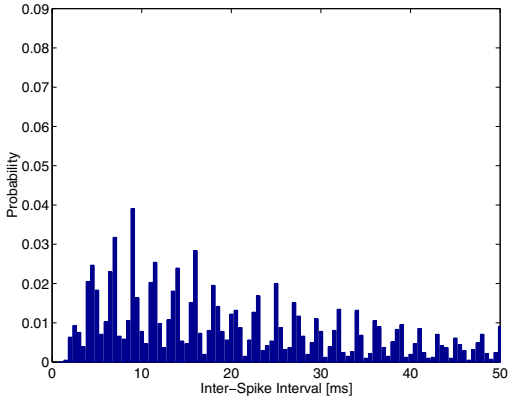

Fig. 7. Inter-Spike Interval histograms with a bin width of 0.5 *ms* at I_p=271 μA ($\hat{\lambda}_{p-spon}$=14 s^{-1}) and f=440 Hz, m=5 %.

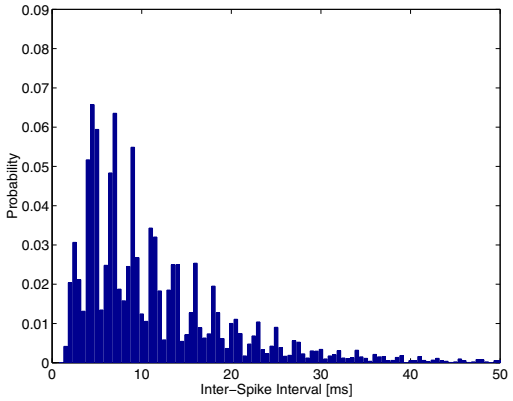

Fig. 8. Inter-Spike Interval histograms with a bin width of 0.5 *ms* at I_p=279 μA ($\hat{\lambda}_{p-spon}$=46 s^{-1}) and f=440 Hz, m=5 %.

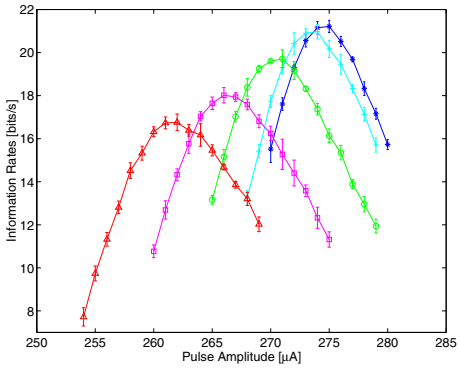

Fig. 9. The relation between the rate of pseudo-spontaneous spikes and the information rate of the spike trains in the ANF model at m=1.0 % with '*', 2.5 % with '+', 5.0 % with 'o', 7.5 % with '□', and 10.0 % with '△', and f =440 Hz.

The information rates as a function of the amplitude of electric pulsatile stimulus currents, I_p, are depicted in Figure 9 at $f = 440Hz$, and the modulation depth m= 1.0 % with '*', 2.5 % with '+', 5.0 % with 'o', 7.5 % with '□', 10.0 % with '△'. The information rate was increased, maximized, and then decreased as the spontaneous rate, i.e., I_p was increased, like a typical curve of the regular stochastic resonance. This result implies a resonance phenomenon dependent on the rate of pseudo-spontaneous spikes, $\hat{\lambda}_{p-spon}$.

IV. CONCLUDING REMARKS

In this proceedings we have reported how the rates of pseudo-spontaneous spikes would affect information transmission of the spike trains in response to the electric pulsatile stimulus currents (electric stimulation) in an auditory nerve fiber (ANF) model through computer simulations. The results show that the information rates increased, reached a maximum, and then decreased as the rate of pseudo-spontaneous spikes increased, implying a resonance phenomenon dependent on the rate of pseudo-spontaneous spikes in electrical stimulation.

It was observed at all cases of pseudo-spontaneous spike rates that the spike firing times were not synchronized well to sinusoidal functions of 440 Hz in raster plots. The ISI histograms were composed of a periodic components of 440 Hz, but of less random components. Nevertheless, it was observed that the information rate was increased, maximized, and then decreased as the pseudo-spontaneous rate was increased, implying a resonance phenomenon dependent on the rate of pseudo-spontaneous spikes at a sinusoidal frequency of 440 Hz and a modulation depth of 1.0, 2.5. 5.0, 7.5, or 10.0 %. However, we note that the rate of pseudo-spontaneous spikes, $\hat{\lambda}_{p-spon}$, which maximizes the information rates was approximately 14 [s^{-1}] at f=440 Hz and m=5 %, being smaller than the spontaneous spike rate reported for acoustic stimulation in animal experiments [6], [7].

In conclusion, these findings would accelerate our understanding of encoding electric stimuli into the spike trains in the ANFs and may play a key role in the design of better cochlear prostheses.

REFERENCES

[1] N. Y. S. Kiang, and E. C. Moxon, "Physiological considerations in artificial stimulation of the inner ear," ***Ann. Otol. Rhinol. Laryngol.***, 81, pp.714-730, 1972.

[2] D. H. Johnson, and N. Y. S. Kiang, "Analysis of discharges recorded simultaneously from pairs of auditory nerve fibers," ***Biophys. J.***, 16, pp. 719-734, 1976.

[3] R. R. Pfeiffer and N. Y. S. Kiang, "Spike Discharge Patterns of Spontaneous and Continuously Stimulated Activity in the Cochlear Nucleus of Anesthetized Cats," ***Biophys. J.***, Vol.5, pp.301-316, 1965.

[4] K. C. Koerber, R. R. Pfeiffer, W. B. Warr, and N. Y. S. Kiang, "Spontaneous Spike Discharges from Single Units in the Cochlear Nucleus after Destruction of the Cochlea," ***Exp. Neurol.***, Vol. 16, pp. 119-130, 1966.

[5] C. H. Molnar and R. F. Pfeiffer, "Interpretation of Spontaneous Spike Discharge Patterns of Neurons in the Cochlear Nucleus," ***Proc. IEEE***, Vol.56, pp.993-1014, 1968.

[6] L. C. Liberman, "Auditory-nerve response from cats raised in a low-noise chamber," ***J. Acoust. Soc. Am.***, 63, pp.442-455, 1978.

[7] L. C. Liberman, "Single-neuron labeling in the cat auditory nerve," ***Science***, 216, pp.1239-1241, 1982.

[8] L. C. Liberman, "Central projections of auditory-nerve fibers of different spontaneous rate I. Anteroventral cochlear nucleus," ***J. Comp Neurol.***, 313, pp.240-258, 1991.

[9] L. C. Liberman, "Central projections of auditory-nerve fibers of different spontaneous rate II. Posteroventral and dorsal cochlear nuclei," ***J. Comp Neurol.***, 327, pp.17-36, 1993.

[10] J.T. Rubinstein, B.S. Wilson, C.C. Finley, C.C. and P.J. Abbas, "Pseudospontaneous activity : stochastic independence of auditory nerve fibers with electrical stimulation," ***Hear. Res.***, 127, pp.108-118, 1999.

[11] L.M. Litvak, Z.M. Smith, B. Delgutte, and D.K. Eddington, "Desynchronization of electrically evoked auditory-nerve activity by high-frequency pulse trains of long duration," ***J. Acoust. Soc. Am.***, 114, pp.2066-2078, 2003.

[12] C. A. Miller, P. J. Abbas, B. K. Robinson, K. V. Nourski, F. Zhang, and F.C. Jeng, "Auditory Nerve Fiber Responses to Combined Acoustic and Electric Stimulation," ***J. Assoc. Res. Otolar.***, Vol.10, pp.425-445, 2019.

[13] P. Kumsa, and H. Mino, "Effects of rates of spontaneous synaptic vesicle secretions in inner hair cells on information transmission in an auditory nerve fiber model," ***34th Annual International Conference of the IEEE EMBS***, pp.2993-2996 , 2012.

[14] H. Mino, J.T. Rubinstein, and J. A. White, "Comparison of Computational Algorithms for the Simulation of Action Potentials with Stochastic Sodium Channels," ***Ann. Biomed. Eng.***, 30, pp.578-587, 2002.

[15] H. Mino, J.T Rubinstein, and C. A. Miller, and P.J.Abbas, "Effects of Electrode-to-Fiber Distance on Temporal Neural Response with Electrical Stimulation," ***IEEE Trans. on Biomed. Eng.***, Vol.51, pp.13-20, 2004.

[16] H. Mino, "Encoding of Information Into Neural Spike Trains in an Auditory Nerve Fiber Model With Electric Stimuli in the Presence of a Pseudospontaneous Activity," ***IEEE Trans. on Biomed. Eng.***, Vol.54, pp.360-369, 2007.

[17] W.H. Press, S.A. Teukolsky, W.T. Vetterling, and B.P. Flannery, ***Numerical Recipes in C : The Art of Scientific Computing***. New York, Cambridge University Press, pp.847-851, 1993.

[18] P. Dayan and L.F. Abbott, ***Theoretical Neuroscience : Computational and Mathematical Modeling of Neural Systems***, The MIT Press, Cambridge, MA, 2001.

[19] R.R. de Ruyter van Steveninck, G.D. Lewen, S.P. Strong, R. Koberle, W. Bialek, "Reproducibility and variability in neural spike trains," ***Science***, 275(5307), pp.1805-1808, 1997.

[20] A. Zador, "Impact of synaptic unreliability on the information transmitted by spiking neurons,"